Ab initio Simulation of Helium-Ion Microscopy Images: The Case of Suspended Graphene

Hong Zhang,[1] Yoshiyuki Miyamoto,[2,*] and Angel Rubio[3]

[1]*College of Physical Science and Technology, Sichuan University, Chengdu 610065, China*

[2]*Graphene Division, Technology Research Association for Single Wall Carbon Nanotubes (TASC), Nanosystem Research Institute, National Institute of Advanced Industrial Science and Technology (AIST), Central 2, 1-1-1 Umezono, Tsukuba, Ibaraki 305-8568, Japan*

[3]*Nano-Bio Spectroscopy group and ETSF Scientific Development Centre, Centro de Física de Materiales CSIC-UPV/EHU-MPC and DIPC, Universidad del País Vasco UPV/EHU, Avenida de Tolosa 72, E-20018 San Sebastian, Spain*

(Received 12 August 2012; revised manuscript received 26 October 2012; published 27 December 2012)

Helium ion microscopy (HIM), which was released in 2006 by Ward *et al.*, provides nondestructive imaging of nanoscale objects with higher contrast than scanning electron microscopy. HIM measurement of suspended graphene under typical conditions is simulated by first-principles time-dependent density functional theory and the 30 keV He^+ collision is found to induce the emission of electrons dependent on the impact point. This finding suggests the possibility of obtaining a highly accurate image of the honeycomb pattern of suspended graphene by HIM. Comparison with a simulation of He^0 under the same kinetic energy shows that electron emission is governed by the impact ionization instead of Auger process initiated by neutralization of He^+.

DOI: 10.1103/PhysRevLett.109.265505 PACS numbers: 61.48.Gh, 68.37.−d, 79.20.Rf, 81.05.U−

The development of nondestructive imaging techniques that provides the maximum amount of information about the structural and dynamical properties of raw nanostructures is of fundamental importance to nanoscience. Scanning electron microscopy (SEM) is a useful nondestructive imaging method performed on a portable apparatus, but the spatial resolution of SEM is not comparable with that of high-resolution transmission electron microscopy (HRTEM), that needs destructive pretreatment of samples. Compared with SEM, helium ion (He^+) microscopy (HIM) [1] produces higher contrast images. The improvement in contrast is achieved by the atomic level ion source, which can generate an ion beam with a diameter three times the ionic diameter of helium by discharge at a sharpened tungsten tip [1]. An even narrower He^+ beam with a diameter of a single ion has also been reported [2]. The HIM measurements of nanostructures are nondestructive unless the flux of the He^+ beam is high, for example, as in etching [3]. The technique is nondestructive because of the small ion-ion collision cross section at a He^+ kinetic energy of around 30 keV, which is the normal operating energy for HIM. Imaging the thinnest known material, graphene, is a particular challenge. Graphene was first isolated in 2004 by the mechanical peeling of highly oriented pyrolytic graphite [4]. It has previously been demonstrated that HIM images of suspended few-layer graphene can be obtained [3]; therefore, we have examined the feasibility of taking HIM images of monolayer graphene.

Usually, HIM images are recorded by detecting secondary emitted electrons, the intensity of which depends on the position of the beam. The emitted electron yield is often higher for HIM than for SEM [1], and the kinetic energy of the emitted electrons is of the order of several electron volts [5]. The higher contrast of HIM compared with SEM [1] has been theoretically analyzed by simulating a 30 keV He^+ ion, which showed a narrower lateral spread compared with heavier ions or electron beams [6,7], and by statistical treatment of the subsequent electron emission [8]. Although these analyses are valuable, a theoretical study of the microscopic mechanisms of secondary electron emission in HIM has not yet been published [9]. This Letter aims to tackle this issue by using a state-of-the-art first-principles modeling technique in the time-dependent density functional theory (TDDFT) framework [11]. This approach can directly monitor electron-ion dynamics on both projectile He^+ and the target graphene sheet upon collision *without adjustable parameters*. Cross sections of interaction between helium 1*s* orbital and graphene valence orbitals, as well as ion-ion, and ion-electron interactions are automatically taken into account with different impact points. To our knowledge, this approach has never been applied to interpret HIM image.

In this Letter, we show that HIM can produce images of a suspended graphene sheet. The simulations suggest that impact ionization is likely to be the main factor that governs the secondary electron emission from the graphene sheet. We have performed an extensive first-principles simulation based on TDDFT for the electron-ion dynamics of He^+ ion collision with a suspended graphene sheet. The simulations were carried out using a supercell with a vacuum thickness of 30 Å [12]. Within this simulation domain, the onset of the electron emission was observed by monitoring the increase of the electron density in the vacuum region from 3 to 9 Å above and below the graphene sheet. The change in the intensity of the emitted electron

pattern depended on the He^+ impact point, such that the honeycomb pattern of graphene could be resolved by HIM. The advantage of the HIM analysis of graphene over HRTEM is that it does not require sample preparation before measurement.

For the TDDFT-molecular dynamics (MD) simulation, it was necessary to prepare the initial electron wave function conditions for the system with He^+ above the graphene sheet. However, the solution of the static Kohn-Sham equation [13] gave the electronic ground state of this system as having a neutral He (He^0), because the level of $1s$ orbital of He^+ was located below the lowest valence band of the graphene. This unnatural initial condition was avoided by individually computing the electronic structure of He^+ and graphene and merging them according to the following procedure. The series of wave functions for He^+, $\{\psi_1^{He^+}(\mathbf{r}, t), \ldots, \psi_n^{He^+}(\mathbf{r}, t)\}$, and its valence charge density, $\rho_{He^+}(\mathbf{r}, t)$, and the series of the wave functions for the graphene sheet, $\{\psi_1^{gr}(\mathbf{r}, t), \ldots, \psi_m^{gr}(\mathbf{r}, t)\}$, and its valence charge, $\rho_{gr}(\mathbf{r}, t)$, were individually computed in the common unit cell. Both He^+ and graphene were located in the same cell with the Hamiltonians made of the sum of the valence charge densities, $\rho_{He^+}(\mathbf{r}, t) + \rho_{gr}(\mathbf{r}, t)$. The distance between the He^+ and the graphene sheet was kept as 15 Å, so the overlap of the wave functions of these objects was negligibly small. Thus, the direct product of the series of valence wave functions, $\{\psi_1^{He^+}(\mathbf{r}, t), \ldots, \psi_n^{He^+}(\mathbf{r}, t), \psi_1^{gr}(\mathbf{r}, t), \ldots, \psi_m^{gr}(\mathbf{r}, t)\}$, was dealt with as an orthonormal set of valence wave functions of the mixed system, with fixed occupation numbers assigned for individual systems. The excite state dynamics within TDDFT only requires the occupied valence wave function. This computational method has previously been used to simulate an Ar^{7+} ion colliding with a graphene sheet [14]. A gradual acceleration technique was used to obtain a velocity of 30 keV for He^+, and to avoid artificial electron excitation inside the He^+ before the collision [14].

The electron-ion dynamics during the He^+ collision with the graphene was described by coupling TDDFT for the electron time evolution with classical MD for the ions (Ehrenfest dynamics [15]) [16], as implemented in the first-principles simulation tool for electron-ion dynamics [17]. The Suzuki-Trotter split operator technique [18] was used for the real-time propagation of the Kohn-Sham wave functions. Periodic boundary conditions were used; therefore a super-cell consisting of a 5×5 graphene unit cell and a vacuum region of 30 Å was used to prevent a sudden charge transfer from the graphene sheet to the He^+ before the TDDFT-MD simulation. The electron-ion interaction was described by norm-conserving pseudopotentials [19]. The local density approximation [20] was employed to describe the exchange-correlation functional form, which was obtained by fitting to the uniform gas calculation [21]. Further details of the computational method are described in Ref. [22]. The low dose of He^+ ion was assumed in this Letter, so series of He^+ impact after electron emission was not considered.

Figures 1(a) and 1(b) show the impact points (labeled as A-F) and snapshots of the height distribution of electrons at $t = 2.9$ fs, when the He^+ is 14 Å away from the sheet. The charge distribution was taken as the planar average. At this time, no significant kinetic energy was transferred to the C atoms of the graphene sheet, because of the very small cross section of the ion-ion interaction for the high incident kinetic energy of He^+ (30 keV). The lower kinetic energy of the He^+ ion should increase the cross section; it should increase significantly when the kinetic energy is below 1 keV [24].

Figure 1(b) also shows that the emitted electron distribution increased from impact points A to F. The depicted contour lines for secondary emitted electrons in Fig. 1 were estimated by interpolating the charge distribution at a height of 8 Å for all the impact points [Fig. 1(c)]. The height is chosen to avoid spurious effects from the periodic boundary conditions used in the present Letter. The charge distribution in the negative region also shows a similar trend in dependence on impact points A-F, but the distribution in this region is influenced by the presence of the He ion. In practice, the intensity of the secondary emitted electron should be measured when the He ion is far from the graphene sheet. At the brightest impact points, the integrated value of the electrons emitted from a height of 3 to 9 Å was 0.29 electrons [25]. Although the emitted electrons did not have a spatial distribution with a sufficient resolution to image the graphene lattice structure, the significant difference in the total amount of electron emission as a function of the impact points of the He^+ beam did

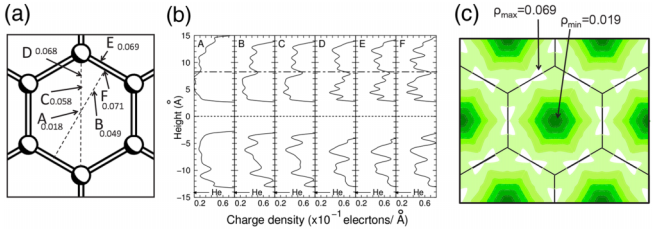

FIG. 1 (color online). (a) Impact points A-F of the He^+ ion. The numbers are the corresponding valence charge (electrons per Å), at a height of 8 Å from the graphene sheet. (b) The distribution of the valence charge density (lateral axis) plotted along the axis normal to the graphene sheet (vertical axis) for impact points A-F. The plots shown in the panels are averaged parallel to the graphene sheet for snapshots at $t = 2.9$ fs when the He atom has already crossed the graphene layer and reached a distance of 14 Å, far from it. The dotted line denotes the graphene sheet, and the dashed-dotted line denotes where the charge density of the emitted electron shows a peak. (c) Contour map of the intensity profile of the secondary emitted electron as a function of the impact points of the helium ion, which produces a HIM image. The maximum and minimum values of the contour lines are shown in electrons per angstrom. The values of the contour lines are on a linear scale.

provide an image [Fig. 1(c)]. The use of pseudopotentials introduces some error in describing the emitted electrons impacting on top of the C atoms; however, as we have to take an average over the beam size, this error is minor in the contrast of the HIM images shown here. The 0.25 nm He^+ beam generated by the atomic level ion source [1] in the HIM scanning mode is larger than the C-C bond length of graphene (0.142 nm) and is comparable with the diagonal distance of the hexagonal rings in the graphene sheet (0.28 nm). Thus, we conclude that a narrower ion beam [2] is necessary for obtaining an image of the honeycomb lattice image derived from our simulations.

Figure 2(a) shows the calculated time evolution of the electron height distribution at impact point E of Fig. 1(a). The scale of the electron density in this figure starts from zero. Before the collision of He^+ with the graphene, no significant charge distribution extended from the graphene or He^+. Near the moment of impact ($t \sim 1.45$ fs) the charge distributions of the graphene and He^+ appeared to merge at 2.18 fs after the impact, and the electrons showed a spatial distribution away from the graphene sheet and remained apart from the graphene sheet at $t = 2.9$ fs, as displayed in Fig. 1(b).

We now analyze the origin of the electron emission displayed in Figs. 1 and 2. When the charge density around the He atom at $t = 2.9$ fs within a radius of 3 Å was partially integrated, the He nucleus acquired 1.2–1.4 electrons, depending on the impact points [27]. This incomplete neutralization of the He ion after passing the graphene sheet suggests a small secondary electron emission started with the neutralization of the He ion [28]. The secondary electron emission by Auger processes including core-shell electrons giving kinetic energy of the order of hundreds of eV is not considered since that kinetic energy is too high compared to the reported values in HIM [5]. The incomplete neutralization is partly caused by the high speed of the He^+ ion, and by the atomic-layer thickness of the graphene sheet. Thus, the interaction time is too short to achieve complete charge transfer. The TDDFT simulation with lower ion speeds [29] showed a larger amount of charge transfer from the graphene sheet [30].

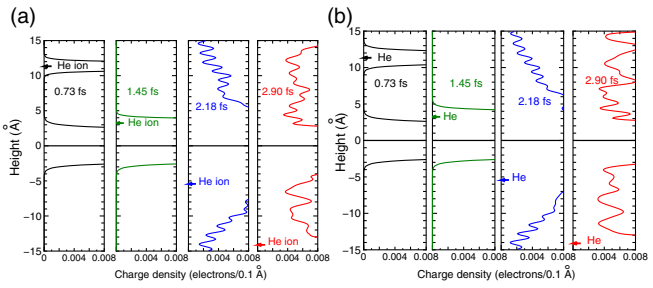

FIG. 2 (color online). (a) Time evolution of the height distribution of the valence charge for the He^+ ion colliding with site E in Fig. 1(a). The height of the graphene was the zero level. The change in the He atom position is indicated by arrows. The He ion lost about 88 eV in kinetic energy; however, this energy-loss introduces a very small change in the He trajectory displayed in this figure. (b) The same simulation starting with a neutral He atom.

The influence of the charge transfer was examined by performing a hypothetical simulation of He^0 colliding with a graphene sheet with a kinetic energy of 30 keV at site E. This produced a similar charge distribution to He^+. Figure 2(b) shows the time evolution of the charge distribution during the impact of the neutral He atom (He^0). The results are also similar to the He^+ impact shown in Fig. 2(a).

During the impact of the He^+ ion, the ion's kinetic energy decreased by around 88 eV, which is a measure of the stopping power due to electron excitation in graphene [24] and in the projectile ion [33].

The high resolution demonstrated by our simulation is still challenging with the current experimental setup, but the similarity of our simulated HIM image with the valence charge profile of graphene [see Fig. 3(a)] allows us to do fast estimations of the experimental HIM images. The smeared image of valance charge density of a graphene edge shown in Fig. 3(b) can show the observed sharpness of the graphene edge [34] consistent with the beam size. We hope the challenge of reaching sub-nm resolution [35] will be achieved soon.

According to our simulation, charge redistribution occurred in the graphene sheet in addition to the impact-induced electron emission in the vacuum region. Figure 3(c)

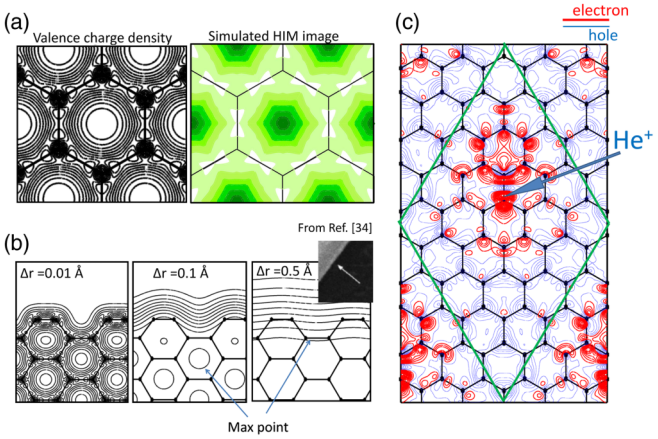

FIG. 3 (color online). (a) Comparison between valence charge density and simulated HIM image, Fig. 1(a). (b) Valence charge density at graphene edge with spatial broadening factor ranging from 0.01 to 0.5 Å, the last one corresponds to the beam diameter of 2 Å. The inset is an experimentally reported HIM image at an edge of highly oriented pyrolytic graphene [34]. (c) Charge redistribution on the graphene sheet for the He^+ ion impact point E at $t = 2.9$ fs. The impact point is denoted by the arrow. The red (thick) and blue (thin) lines are contour maps for electrons and holes, respectively. The maximum quantity of the contour lines for holes is 0.0067 $e/(\text{Bohr rad})^3$, whereas that of the contour lines for electrons is 0.024 $e/(\text{Bohr rad})^3$, with a linear interval of 0.000 67$e/(\text{Bohr rad})^3$.

shows the charge redistribution in the graphene sheet calculated by subtracting the charge density before the He^+ collision ($t = 0$ in the TDDFT-MD simulation) from the charge density at $t = 2.9$ fs with impact point E in Fig. 1(a). Interestingly, the electron accumulation near the impact point implies that when He^+ was passing through the graphene the electrons were attracted to the ion. However, this was not large enough to complete the neutralization. We expect that this charge redistribution will be rapidly neutralized when the graphene sheet is held in place by a conducting material or when an electron flood gun is used [36], and that this neutralization will not structurally damage the graphene. Furthermore, the residual forces on the C atoms at this moment are in the order of 0.01 HR/au which can cause vibrations but will not break the C-C bonds because the heat is dissipated. Thus, we expect that the HIM measurements will be nondestructive [37].

In conclusion, we predict that resolution of HIM could be competitive to HRTEM when highly focused ion beam technology [2] is applied and measuring a lattice image of suspended graphene by HIM is feasible. The first-principles electron-ion dynamics simulation revealed that an image constructed from secondary emitted electrons, which strongly depended on the impact point of the He^+ ion, displays the honeycomb pattern of graphene. Increase of precision of the contour line will be useful for examining future available experimental data with higher resolution. The impact ionization of graphene was predicted to be the mechanism of electron emission from single-layer graphene by comparing of the simulation of the He^0 and the He^+ collisions. Slowing down He^+ may increase the probability of He neutralization, resulting in Auger electron emission, although this would also increase the cross section of the ion-ion interaction and damage the graphene sheet. We expect that the presented mechanism of HIM imaging is not specific but will be applicable for other materials.

Atomic level resolution of suspended graphene has been achieved by scanning tunneling microscope (STM) [38–40]. One advantage of HIM is its nondestructive nature with a low dose of He ions while STM needs high attention in operating the tip to avoid mechanical interaction and subsequent oscillation on the graphene sheet [41]. Both STM and HIM are very sensitive to contamination of the graphene sheet, which influences the valence electronic structure and therefore the corresponding STM and HIM images.

All calculations were performed on the Earth Simulator. H. Z. acknowledges financial support from the National Natural Science Foundation of China (NSFC Grant No. 11074176 and NSAF Grant No. 10976019) and support from the Research Fund for the Doctoral Program of Higher Education of China (Grant No. 20100181110080). Y. M. acknowledges funding from the Strategic Programs for Innovative Research (SPIRE), MEXT, the Computational Materials Science Initiative (CMSI), Japan, and support from the Research Organization of Information Science and Technology (RIST), Tokyo. A. R. acknowledges funding from the European Research Council Advanced Grant DYNamo (ERC-2010-AdG -Proposal No. 267374), Spanish Projects (No. FIS2010-21282-C02-01 and No. PIB2010US-00652), Grupos Consolidados UPV/EHU del Gobierno Vasco (IT-319-07), Ikerbasque and SGIker ARINA (UPV/EHU), and CRONOS (Contract No. 280879-2).

*yoshi-miyamoto@aist.go.jp

[1] B. W. Ward, J. A. Notte, and N. P. Economou, J. Vac. Sci. Technol. B **24**, 2871 (2006).
[2] M. Rezeq, J. Pitters, and R. Wolkow, J. Chem. Phys. **124**, 204716 (2006).
[3] M. C. Lemme, D. C. Bell, J. R. Williams, L. A. Stern, B. W. H. Baugher, P. Jarillo-Herrero, and C. M. Marcus, ACS Nano **3**, 2674 (2009).
[4] K. S. Novoselov, A. K. Geim, S. V. Morozov, D. Jiang, Y. Zhang, S. V. Dubonos, I. V. Grigorieva, and A. A. Fisov, Science **306**, 666 (2004).
[5] L. Scipioni, C. A. Sanford, J. Notte, B. Thompson, and S. McVey, J. Vac. Sci. Technol. B **27**, 3250 (2009).
[6] D. Cohen-Tanugi and N. Yao, J. Appl. Phys. **104**, 063504 (2008).
[7] S. Sijbrandij, J. Notte, C. Sanford, and R. Hill, J. Vac. Sci. Technol. B **28**, C6F6 (2010).
[8] K. Ohya, Nucl. Instrum. Methods Phys. Res., Sect. B **206**, 52 (2003).
[9] The interaction of He^+ with a solid surface has been investigated [10], although this study used low He^+ transport energies of around 250 eV.
[10] D. L. Bixler, J. C. Lancaster, F. J. Kontur, P. Nordlander, G. K. Walters, and F. B. Dunning, Phys. Rev. B **60**, 9082 (1999).
[11] E. Runge and E. K. U. Gross, Phys. Rev. Lett. **52**, 997 (1984).
[12] A vacuum region of over 30 Å caused numerical instability in preserving a self-consistent potential field and the Kohn–Sham orbitals in the TDDFT time evolution.
[13] W. Kohn and L. J. Sham, Phys. Rev. **140**, A1133 (1965).
[14] Y. Miyamoto and H. Zhang, Phys. Rev. B **77**, 045433(E) (2008); **77**, 079903 (2008).
[15] P. Ehrenfest, Z. Phys. **45**, 455 (1927).
[16] See the recent developments in adiabatic and nonadiabatic dynamic processes in TDDFT detailed in M. A. L. Marques, N. Maitra, F. Nogueira, E. K. U. Gross, and A. Rubio, *Fundamentals of Time Dependent Density Functional Theory*, Lecture Notes in Physics Vol. 837 (Springer, New York, 2011).
[17] O. Sugino and Y. Miyamoto, Phys. Rev. B **59**, 2579 (1999); O. Sugino and Y. Miyamoto, Phys. Rev. B **66**, 089901(E) (2002).
[18] M. Suzuki, J. Phys. Soc. Jpn. **61**, 3015 (1992).
[19] N. Troullier and J. L. Martins, Phys. Rev. B **43**, 1993 (1991).
[20] J. P. Perdew and A. Zunger, Phys. Rev. B **23**, 5048 (1981).

[21] D. M. Ceperley and B. J. Alder, Phys. Rev. Lett. **45**, 566 (1980).

[22] Further technical details of the calculation: calculations with only a Γ point and three irreducible *k*-points, including the *K* point, were compared for the 5×5 unit cell for the momentum-space integration. The Γ only calculation was also performed with a 7×7 cell. In both cases, the electron emission was similar, thus a 5×5 cell with a Γ point is sufficient. A plane-wave cutoff energy of 60 Ry was chosen to guarantee good convergence of the electronic wave functions and the Hellmann–Feynman forces with the previous set of parameters. According to high precision calculations, the interactions between the molecules and the graphitic materials are small [23] compared to the 30 keV incident kinetic energy of the He^+ ion. Therefore, the choice of exchange-correlation functional should not influence the results.

[23] X. Ren, A. Tkatchenko, P. Rinke, and M. Scheffler, Phys. Rev. Lett. **106**, 153003 (2011).

[24] A. V. Krasheninnikov, Y. Miyamoto, and D. Tománek, Phys. Rev. Lett. **99**, 016104 (2007).

[25] The current simulation was within a time constant of up to 2.9 fs; therefore, the complete emission was not simulated. However, the distribution of the electrons around 8 Å above the graphene sheet strongly suggests the nonbonding nature of these electrons, because the self-consistent potential profile reaches to the vacuum level beyond 3 Å above the graphene sheet [26].

[26] H. Min, B. Sahu, S. K. Banerjee, and A. H. MacDonald, Phys. Rev. B **75**, 155115 (2007).

[27] In TDDFT, the fractional number of an electron on a He atom can be interpreted as the probability of neutralization, which ranges from 20% to 40%, depending on the impact point.

[28] The Auger process should be described by a two-particle representation for electron wave functions; therefore, TDDFT using a single particle representation for the electron wave function requires careful treatment.

[29] T. Kubota, N. Watanabe, S. Ohtsuka, T. Iwasaki, K. Ono, Y. Iriye, and S. Samukawa, J. Phys. D **44**, 125203 (2011).

[30] The adiabatic exchange-correlation scheme employed in our simulation restricts the electron-electron interaction as elastic. This restriction may cause an artificial Rabi oscillation, which would suppress the complete charge transfer to the He^+ ion [31,32], although this oscillation is typical in systems with very few electrons.

[31] N. Helbig, J. I. Fuks, I. V. Tokatly, H. Appel, E. K. U. Gross, and A. Rubio, Chem. Phys. **391**, 1 (2011).

[32] J. I. Fuks, N. Helbig, I. V. Tokatly, and A. Rubio, Phys. Rev. B **84**, 075107 (2011).

[33] Y. Miyamoto and H. Zhang, Phys. Rev. B **77**, 161402(R) (2008).

[34] R. Hill and F. H. M. Faridur Rahman, Nucl. Instrum. Methods Phys. Res., Sect. A **645**, 96 (2011).

[35] M. T. Postek and A. E. Vladár, Scanning **30**, 457 (2008).

[36] M. T. Postek, A. E. Vladár, and B. Ming, in *Frontiers of Characterization and Metrology for Nanoelectronics: 2009 International Conference on Frontiers of Characterization and Metrology for Nanoelectronics: Albany, New York*, edited by D. Seiler *et al.*, AIP Conf. Proc. No. 1173 (AIP, New York, 2009).

[37] See Supplemental Material at http://link.aps.org/supplemental/10.1103/PhysRevLett.109.265505 for time evolution of the force field acting on the carbon atom closest to the He^+ ion passing through impact point *E* in Fig. 1(a). The solid (red) line shows the parallel force in the sheet, and the positive and negative directions are closer to and farther from the impact point, respectively. The dotted (green) curve shows the force field in the normal direction to the graphene sheet, and the positive and negative directions indicate the incoming and outgoing directions of the He^+ ion.

[38] N. N. Klimov, S. Jung, S. Zhu, T. Li, C. Alan Wright, S. D. Solares, D. B. Newell, N. B. Zhitenev, and J. A. Stroscio, Science **336**, 1557 (2012).

[39] P. Xu, Y. Yang, S. D. Barber, M. L. Ackerman, J. K. Schoelz, D. Qi, I. A. Kornev, L. Dong, L. Bellaiche, S. Barraza-Lopez, and P. M. Thibado, Phys. Rev. B **85**, 121406(R) (2012).

[40] R. Zan, C. Muryn, U. Bangert, P. Mattocks, P. Wincott, D. Vaughan, X. Li, L. Colombo, R. S. Ruoff, B. Hamilton, and K. S. Novoselov, Nanoscale **4**, 3065 (2012).

[41] A weak point of HIM may be noise coming from further emitted electrons caused by excessive collision of traversing the He ion to surrounding material that could be avoided by taking the proper geometrical setup throughout the measurement.